JOC The Journal of Organic Chemistry
Article
pubs.acs.org/joc

Comparative Reaction Diagrams for the S_N2 Reaction Formulated According to the Leffler Analysis and the Hammond Postulate

Robert C. Haddon,[*,†] Ziqi Tian, and De-en Jiang[*]

Chemistry Department and Chemical Engineering Department, University of California, Riverside, California 92521, United States

S Supporting Information

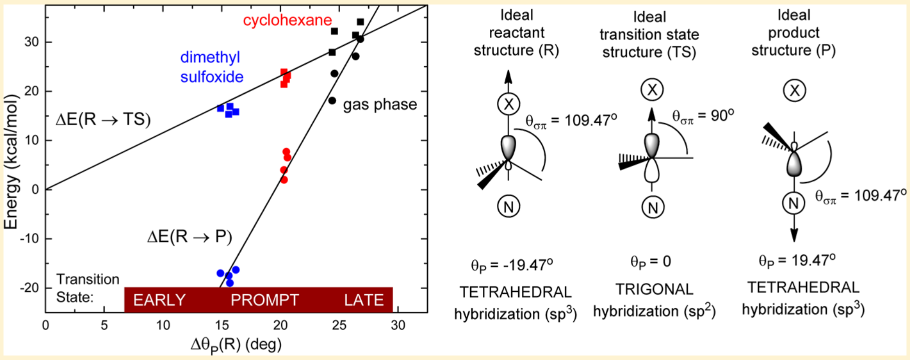

ABSTRACT: The Hammond Postulate and the Leffler analysis have provided a cornerstone in the understanding of reaction processes in organic chemistry for over 60 years, yet quantitative applications of these methodologies over the range of reactions envisaged in the original works remain elusive. In the present paper, we analyze a series of S_N2 reactions in three solvents that lead to endothermic and exothermic reaction processes, and we show that within the hybridization reaction coordinate the S_N2 reaction is fully consistent with both treatments. We give new presentations of the reaction energies as a function of reaction progress, which allow the generation of unified reaction coordinate diagrams that show a linear relationship between the hybridization metric of reaction progress and the relative energies of the stationary points on the potential surface as a function of structure and solvent as originally envisaged by Leffler and Hammond.

■ INTRODUCTION

We take as a modern statement of the Hammond Postulate, "The structure of a transition state resembles the structure of the nearest stable species. Transition states for endothermic steps structurally resemble products, and transition states for exothermic steps structurally resemble reactants."[1] An important implication is the correlation between reaction rates and the positions of equilibria. The paper by Hammond postulates a qualitative relationship between structure and energy along a reaction coordinate,[2] whereas the work by Leffler titled "Parameters for the Description of Transition States",[3] suggests a quantitative (linear) relationship between the changes in the free energies of the transition state, reactants, and products as a function of an independent variable such as solvent or structure, but neither author defines a reaction coordinate with which to gauge structural evolution along the reaction pathway.

The S_N2 reaction has been the subject of a number of previous theoretical studies,[4−14] many of which follow the usual practice of defining the transition state in terms of the internuclear distances involved in the bond breaking and forming steps at the reacting carbon atom. These studies have led to an in-depth understanding of this reaction, and in the present work we consider a series of representative S_N2 methyl transfer reactions (Scheme 1)[7] from the standpoint of the hybridization reaction metric of reaction progress.[15] As we show below, these reactions are particularly appropriate in the present connection as the they span a broad range of exo- and endothermicities as a function of substrate and solvent.[3]

Scheme 1. Methyl Transfer S_N2 Reactions[a,7]

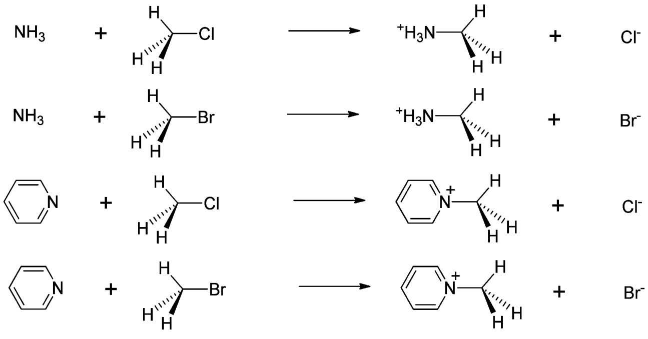

[a]Solvents: (1) gas phase, (2) cyclohexane, and (3) dimethyl sulfoxide

Received: February 10, 2016
Published: April 11, 2016

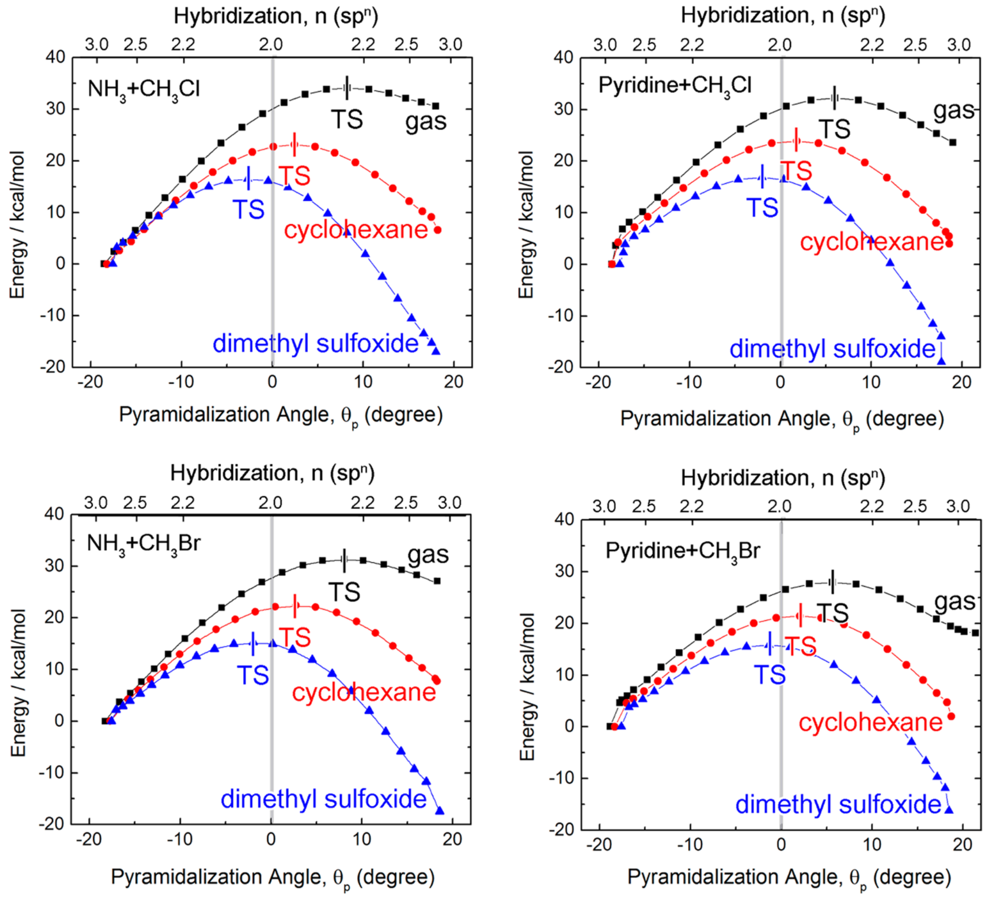

Figure 1. Reaction diagrams calculated for the processes shown in Scheme 1; the reaction coordinate is given by the pyramidalization angle (θ_P, deg) at the methyl group, which determines the hybridization (Figure 2).[15,21]

RESULTS

The potential energy calculations were carried out with the Gaussian 09 program[16] using the SMD solvent model[17] at the M06/6-311+G(d,p) level of theory; transition states were first located and then used to find the reaction profile by following the intrinsic reaction coordinate (Supporting Information (SI)).[18−20] In Figure S1, the reaction progress is a function of the internuclear distances to the methyl group in which the reaction coordinate is taken to be the difference between the bond lengths of the bonds broken and formed in the reaction in the sense that the reactants lie at negative values and the products at positive values of the reaction coordinate.[7] On the basis of a literal interpretation of this definition, all of the reactions would be classified as occurring via late (product-like) transition states.[7]

In Figure 1, the reaction coordinate is taken as the pyramidalization angle (θ_P) at the methyl group (which is a function of the hybridization of that carbon atom, Figure 2) in the sense that reactants lie at negative values and the products lie at positive values of the reaction coordinate (θ_P).[15] The hybridization metric of reaction progress is predicated on the idea that the reaction coordinate should provide an absolute measure of the location of a given structure with respect to the reactants and products in the spirit of the Hammond Postulate:[15] transition states for endothermic steps structurally resemble products, and transition states for exothermic steps structurally resemble reactants.[1]

For S_N2 reactions, the ideal state of the methyl group in the reactants (R) and products (P) is sp^3 hybridization ($|\theta_P|$ = 19.47°), whereas for the transition state (TS), it is sp^2 hybridization ($\theta_P = 0$) (Figure 2). On this basis, all of the gas phase reactions are classified as occurring via late transition states as shown in Figure 1 because they occur beyond planarity (positive transition state pyramidalization angle, θ_P) and the point of sp^2 hybridization of the reacting carbon atom (Table S1). This is in accordance with the Hammond Postulate as the structures are closer to that of the products and the gas phase reactions are strongly endothermic; furthermore, the degree of endothermicity monotonically follows the pyramidalization angles and hybridizations. The reactions in dimethyl sulfoxide (DMSO) are exothermic, and the pyramidalization angles suggest that they are closer to the structure of the reactants in accordance with the Hammond Postulate (negative θ_P at the transition state); in this case, the spread of the transition state pyramidalization angles is small (approximately 1°), as is the variation in the exothermicities of the reactions. The reactions in cyclohexane are weakly endothermic, and the spread in transition state pyramidalization angles is minimal (1°). The transition state pyramidalization angles themselves are also small for this reaction ($\theta_P \approx 2°$), and they show positive values, but of smaller magnitude, than those found in the gas phase reactions as expected from the relative endothermicities of the S_N2 processes in the two reaction media.

Thus, we conclude that, within the framework of the hybridization reaction coordinate, the Hammond Postulate is directly applicable to the S_N2 reaction. As may be seen in

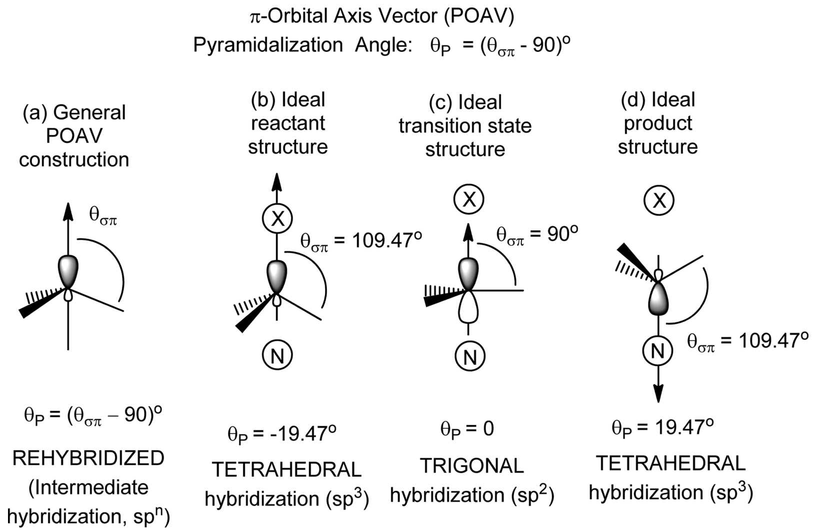

Figure 2. π-Orbital axis vector (POAV), pyramidalization angle (θ_P), and construction for the S_N2 reaction, where N represents the nucleophile (ammonia, pyridine), and X represents the leaving group (Cl, Br). (a) The POAV is that vector that makes equal angles to the three σ-bonds at a tricoordinate carbon atom; the hybridization of the carbon atom follows analytically (sp^n, $n = 2/(1 - 3\sin^2\theta_P)$).[15,21−23] Ideal pyramidalization angles and hybridizations for the S_N2 reaction: (b) reactant (R), (c) transition state (TS), (d) product (P); the reactant pyramidalization angle is defined to be negative.

Figure 1, this metric rigorously divides the reactions between endo- and exothermic processes based purely on the positions of their transition states on the reaction coordinate, thereby directly correlating the rates and positions of equilibria in the S_N2 reaction. As far as we are aware, there are no other published cases where the reaction coordinate is able to provide an absolute measure of reaction progress that fully reproduces the objectives of the Hammond and Leffler articles.[2,3] The idealizations in Figure 1 of the Hammond paper[2] parallel the results in the reaction profiles shown here in Figure 1, which could be combined into a single reaction diagram to allow a direct comparison of the effect of structure and solvent on the reaction processes (which is not possible with the reaction coordinate utilized in Figure S1),[15] thereby allowing the realization of the original intent of the analyses. However, such a diagram would become much too cluttered to be useful when applied to the broad range of organic reactions that are available. Below, we focus on an analysis of the stationary points of the various reactions as a function of the hybridization reaction coordinate within the Leffler and Hammond approaches.

■ DISCUSSION

The analysis by Leffler suggests a linear relationship between the change in free energies of the reactants (ΔG_R), products (ΔG_P), and transition states (ΔG_{TS}) as a function of some variation in the reaction conditions, such as structure or solvent.[3] Thus, the reaction processes studied herein (Scheme 1) constitute an ideal test set for the examination of these relationships, which to our knowledge have never received direct quantitative examination (apart from ref 15).

Leffler argued that the transition state should be intermediate between the reactant and product in some of its properties, in which case it is appropriate to use a linear combination of the properties of the reactants and products to represent the transition state of a reaction.[3] Thus, he used the following approximation to represent the change in free energy of the transition state as a function of an independent variable

$$\Delta G_{TS} = \alpha \Delta G_P + (1 - \alpha)\Delta G_R \tag{1}$$

He went on to suggest that the transition state will resemble the product less when it resembles the reactant more, and thus in eq 1, α represents the resemblance to the product whereas $(1 - \alpha)$ measures the resemblance to the reagent. Hence, the properties of the transition state are regarded as a hybrid between the reactant and product states, and this leads to the following relationship between the activation energy ($\Delta G(R \rightarrow TS) = \Delta G_{TS} - \Delta G_R$) and the free energy change of the reaction ($\Delta G(R \rightarrow P) = \Delta G_P - \Delta G_R$), where these energies and structures are referenced to the reactant, and C is a constant[3]

$$\Delta G(R \rightarrow TS) = \alpha \Delta G(R \rightarrow P) + C \tag{2}$$

This relationship basically puts the Hammond Postulate in quantitative form and suggests a functional relationship between the kinetics and thermodynamics of such reactions. However, in common with the Hammond Postulate, the Leffler analysis did not define the geometric variable (reaction coordinate) that can linearly represent the transition state structure as a hybrid of the reactant and product structures throughout the reaction process. We have previously noted some of the difficulties associated with defining this quantity, particularly where the definition is chosen as a function of the internuclear distances involved in the bond breaking and bond making processes of simple reactions.[15] Below, we consider the use of the hybridization metric of reaction progress as a measure of the geometric variable or reaction coordinate.[15] The hybridization metric of reaction progress (in the form of the pyramidalization angle)[15] provides a natural way to express the structure of the transition state as a hybrid of the reactant and product states, and it is straightforward to directly plot $\Delta E(R \rightarrow TS)$ and $\Delta E(R \rightarrow P)$ versus $\Delta\theta_P(R)$ as a test of eq 2 (Figure 3, where $\Delta\theta_P(R)$ denotes the change in pyramidalization angle from the reactant value).

Figure 3 shows that an excellent correlation exists between the stationary points on the potential surfaces of the reactions and the change in the hybridization metric of reaction progress. This is a particularly important result because it shows that the

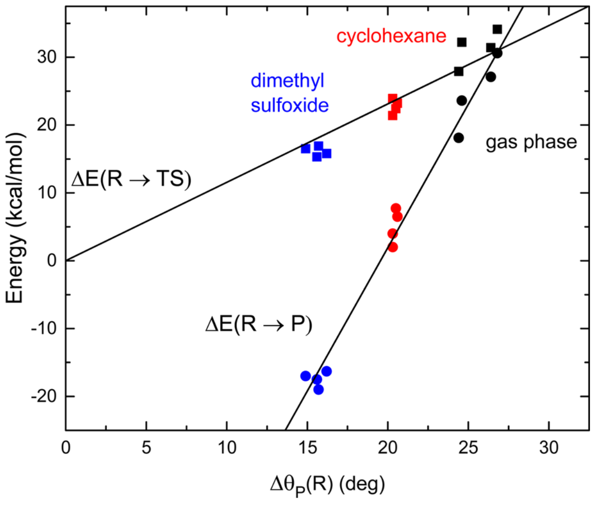

Figure 3. Calculated activation $\Delta E(\mathrm{R} \rightarrow \mathrm{TS})$ and reaction $\Delta E(\mathrm{R} \rightarrow \mathrm{P})$ energies as a function of the reaction progress from the reactant, $\Delta\theta_\mathrm{P}(\mathrm{R}) = (\theta_\mathrm{P}(\mathrm{TS}) - \theta_\mathrm{P}(\mathrm{R}))$,[15] where R = reactants, TS = transition state, and P = products. The energies are given with respect to those of the reactants; the correlation coefficients (R^2) are 0.993 (R → TS) and 0.99 (R → P); the gradients are 1.156 (R → TS) and 4.228 (R → P), and the intercept is −82.6 kcal/mol (R → P). Thus, in analogy with eq 2, we use $\Delta E(\mathrm{R} \rightarrow \mathrm{TS}) = \alpha\, \Delta E(\mathrm{R} \rightarrow \mathrm{P}) + \mathrm{C}$ for which the data here gives $\alpha = 0.273$ and C = 22.6 kcal/mol.

transition state, reactant, and product structures are linearly related by the hybridization of the reacting carbon atom (eq 3); on the basis of Figure 3, we take straight line fits as

$$\begin{aligned}\Delta E(\mathrm{R} \rightarrow \mathrm{TS}) &= M_{\mathrm{R}\rightarrow\mathrm{TS}}\Delta\theta_\mathrm{P}(\mathrm{R})\\ \Delta E(\mathrm{R} \rightarrow \mathrm{P}) &= M_{\mathrm{R}\rightarrow\mathrm{P}}\Delta\theta_\mathrm{P}(\mathrm{R}) + \mathrm{C}'\end{aligned} \tag{3}$$

Thus

$$\begin{aligned}\Delta E(\mathrm{R} \rightarrow \mathrm{TS}) &= (M_{\mathrm{R}\rightarrow\mathrm{TS}}/M_{\mathrm{R}\rightarrow\mathrm{P}})[\Delta E(\mathrm{R} \rightarrow \mathrm{P}) - \mathrm{C}']\\ &= \alpha[\Delta E(\mathrm{R} \rightarrow \mathrm{P}) - \mathrm{C}']\\ &= \alpha\Delta E(\mathrm{R} \rightarrow \mathrm{P}) + \mathrm{C}\end{aligned} \tag{4}$$

where M is the gradient, $\alpha = (M_{\mathrm{R}\rightarrow\mathrm{TS}}/M_{\mathrm{R}\rightarrow\mathrm{P}})$, and $\mathrm{C} = -\alpha\mathrm{C}'$, which reproduces the Leffler relationship (eq 2); for the data in Figure 3, $\alpha = 0.273$ and C = 22.6 kcal/mol. Eq 4 is in the form of eq 2 and allows us to obtain eq 5, which recovers the original Leffler result (eq 1)

$$\Delta E_\mathrm{TS} = \alpha\Delta E_\mathrm{P} + (1 - \alpha)\Delta E_\mathrm{R} \tag{5}$$

There is a natural differentiation between exothermic, thermoneutral, and endothermic reaction processes, which is made apparent in the diagram, as envisaged by Leffler and Hammond. Thus, with the accumulation of more data, it will be possible to specify, based on the structure implicit in the hybridization metric, exactly what is meant by the terms early, prompt, and late transition states, and this point is taken up below in connection with Figure 4.

The analysis supports the thermodynamic interpretation of the parameter α (eqs 1 and 2 and Figure 3) provided by Leffler, but as noted by other authors,[24,25] it seems impossible to relate α to reaction progress. The hybridization metric provides an absolute measure of reaction progress, so it is not surprising to find that α is constant within this analysis even though the stationary points are widely distributed with respect to this reaction coordinate. Nevertheless, the relationships of the structures of the transition states to those of the reactants and products are critical issues for both the Leffler analysis and the Hammond Postulate, and the viability of this relationship is of great importance to the practice of organic chemistry. The hybridization metric provides a simple relationship between these structures based on dynamic rehybridization along the reaction coordinate, which may be readily expressed in terms of a simple geometrical variable—the pyramidalization angle at the carbon atom undergoing the reaction (see, however, ref 26). It is in this sense that the Leffler approximation is satisfied,[3] "We approximate the transition state by regarding it as a hybrid between the reagent and product states."

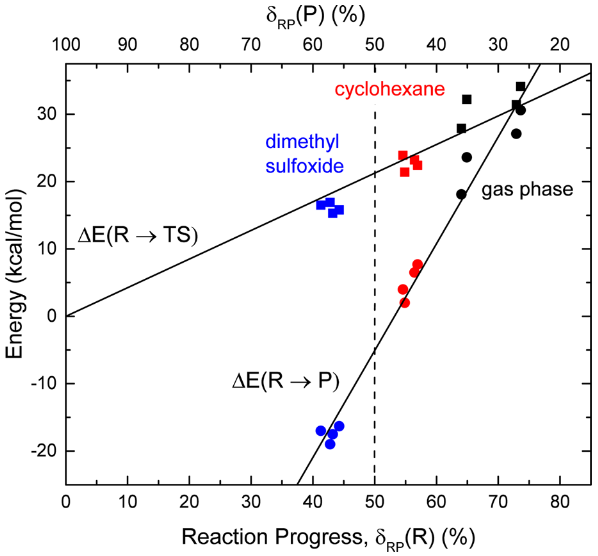

Figure 4. Calculated activation $\Delta E(\mathrm{R} \rightarrow \mathrm{TS})$ and reaction $\Delta E(\mathrm{R} \rightarrow \mathrm{P})$ energies expressed as a function of the structural degree of reaction progress, $\delta_\mathrm{RP}(\mathrm{R})$ % (eq 6) and $\delta_\mathrm{RP}(\mathrm{P})$ % (eq 7), where R = reactants, TS = transition state, and P = products (compare with Figure 3 and Figure S3). If $\Delta\theta_\mathrm{P}(\mathrm{R})$ in eq 3 is replaced by $\delta_\mathrm{RP}(\mathrm{R})$, then the subsequent analysis gives correlation coefficients (R^2) of 0.992 (R → TS) and 0.98 (R → P), gradients of 0.425 (R → TS) and 1.586 (R → P), an intercept of −84.4 kcal/mol (R → P), $\alpha = 0.268$, and C = 22.6 kcal/mol. The results of this analysis are very close to those found in connection with Figure 3, because for this series of reactions (Scheme 1), $|\theta_\mathrm{P}(\mathrm{R})| \approx \theta_\mathrm{P}(\mathrm{P}) \approx 19.47°$, the ideal tetrahedral angle (see Figure 2 and Table S1), and thus, $(\theta_\mathrm{P}(\mathrm{P}) - \theta_\mathrm{P}(\mathrm{R}))$ is almost a constant. In the case of the pericyclic reactions analyzed previously,[15] the analysis associated with Figure 3 gives $\alpha = 0.525$ and C = 36.6 kcal/mol, whereas the treatment in Figure 4 gives $\alpha = 0.411$ and C = 36.5 kcal/mol.

Although we cannot confirm the relationship of α to the structural progress of the reaction as suggested by Leffer,[3] it is possible to define a structural degree of reaction progress that is analogous to the quantity sought by Leffler, but based on the pyramidalization reaction metric shown in Figure 3. This may be accomplished by simply renormalizing $\Delta\theta_\mathrm{p}(\mathrm{R})$ by the total change in the pyramidalization angle for the reaction; thus, we define a structural degree of reaction progress (RP) from the reactant (eq 6) and product (eq 7)

$$\delta_\mathrm{RP}(\mathrm{R}) = \frac{\Delta\theta_\mathrm{P}(\mathrm{R})}{[\theta_\mathrm{P}(\mathrm{P}) - \theta_\mathrm{P}(\mathrm{R})]} = \frac{[\theta_\mathrm{P}(\mathrm{TS}) - \theta_\mathrm{P}(\mathrm{R})]}{[\theta_\mathrm{P}(\mathrm{P}) - \theta_\mathrm{P}(\mathrm{R})]} \tag{6}$$

$$\delta_{RP}(P) = [1 - \delta_{RP}(R)] = \frac{[\theta_P(P) - \theta_P(TS)]}{[\theta_P(P) - \theta_P(R)]} \qquad (7)$$

The degree of reaction progress from the reactant, $\delta_{RP}(R)$, is conveniently expressed as a percentage in Figure 4; this plot is readily interpreted in terms of early (dimethyl sulfoxide) and late (cyclohexane and gas phase) transition states as discussed in connection with Figure 1. Thus, we can paraphrase Leffler[3] and state that the parameter $\delta_{RP}(R)$ measures the resemblance to the product and has 0 and 1 as limits, whereas $\delta_{RP}(P) = [1 - \delta_{RP}(R)]$ measures the resemblance to the reagent (see Figure 4).

Although the foregoing treatment is consistent with the Leffler analysis (Figures 3 and 4), there is an alternative mode of presentation. The Leffler analysis is referenced to the reactant, whereas the Hammond Postulate focuses on the transition state; hence, in Figure 5 we set the transition states as the reference point with respect to energy and structure, and thus, we plot $\Delta E(R \leftarrow TS)$ versus $\Delta\theta_P(R \leftarrow TS)$ and $\Delta E(TS \rightarrow P)$ versus $\Delta\theta_P(TS \rightarrow P)$ (see also Figure S3 for the analysis in terms of $\delta_{RP}(TS)$).

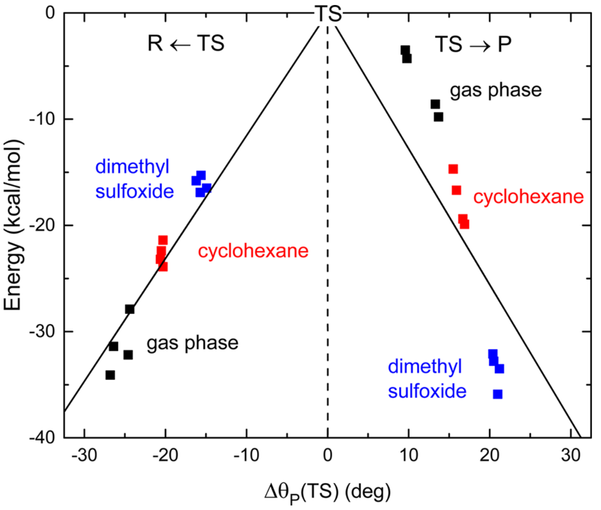

Figure 5. Calculated activation $\Delta E(R \leftarrow TS)$ and reaction $\Delta E(TS \rightarrow P)$ energies (referenced to the transition state) as a function of the change in the measure of reaction progress, $\Delta\theta_p(TS) = (\theta_P(R) - \theta_P(TS))$ and $(\theta_P(P) - \theta_P(TS))$, respectively, where R = reactants, TS = transition state, and P = products; note that this analysis is recast in terms of $\delta_{RP}(TS)$ in Figure S3. The energies are given with respect to those of the transition states; the correlation coefficients (R^2) are 0.993 (R ← TS) and 0.91 (TS → P), and the gradients are 1.156 (R ← TS) and −1.279 (TS → P).

This produces a volcano plot and provides a simple geometric interpretation of the Hammond Postulate in which it is possible to immediately delineate the position of the reactants and products on the potential surface, providing that the gradients of the linear fits (eq 8) are of equal magnitude but opposite sign.

$$\begin{aligned} \Delta E(TS \rightarrow R) &= M_{TS\rightarrow R}\Delta\theta_P(R) \\ \Delta E(TS \rightarrow P) &= M_{TS\rightarrow P}\Delta\theta_P(R) \end{aligned} \qquad (8)$$

From the data in Figure 5, we find $M_{(TS\rightarrow R)} = M_{(R\rightarrow TS)} = 1.156$ (standard error of 0.03) and $M_{(TS\rightarrow P)} = -1.279$ (0.12), and thus, the magnitudes of the slopes agree within the standard errors. Figure 5 graphically presents the structural relationship of the transition states to the reactants and products (see Figure S3) and fulfills the promise of the Hammond Postulate, "The structure of a transition state resembles the structure of the nearest stable species. Transition states for endothermic steps structurally resemble products, and transition states for exothermic steps structurally resemble reactants."[1]

■ CONCLUSIONS

In summary, we have delineated a series of simple analyses that realize for the first time the full promise of the Leffler and Hammond approach to the structures of the transition states of organic chemical reactions and the relationship of the kinetics and thermodynamics of these processes. Our analysis succeeds where other approaches have failed because it is based on the adoption of a well-defined metric for the reaction coordinate in the form of a geometrical parameter (pyramidalization angle) that bears an analytical relationship to the hybridization of the reacting carbon atom.[15] Although this paper has focused on the S_N2 reaction, it is important to note that the hybridization reaction metric is general within organic chemistry and is applicable to most carbon-based chemical reaction processes, including additions, eliminations, substitutions, rearrangements, and radical reactions—all of which involve the rehybridization of a carbon atom along the reaction pathway.[15] The pyramidalization angle has been widely applied to distorted π-electron systems,[27] fullerenes,[28] and carbon nanotubes,[29] and the present analysis is readily extendable to other arenas that encompass carbon bond-forming processes, such as catalysis. The hybridization reaction coordinate offers a unified viewpoint of a very large group of organic chemical reactions that will facilitate direct comparisons between many seemingly disparate processes according to the Leffler and Hammond analyses.

Finally, we emphasize the complementary nature of the relationship between the hybridization metric and the use of some function of the bonds broken and formed as a reaction coordinate: the latter treatment is appropriate for the *control* of structures on a potential surface, whereas the hybridization metric is useful as an *indicator* of reaction progress.[15]

■ ASSOCIATED CONTENT

Ⓢ Supporting Information

The Supporting Information is available free of charge on the ACS Publications website at DOI: 10.1021/acs.joc.6b00298.

Methods, stationary point structures, and energies (PDF)

■ AUTHOR INFORMATION

Corresponding Authors

*E-mail: haddon@ucr.edu.
*E-mail: de-en.jiang@ucr.edu.

Notes

The authors declare no competing financial interest.

†Deceased April 21, 2016.

■ REFERENCES

(1) McMurry, J. *Organic Chemistry*; Brooks/Cole: Pacific Grove, 1995.
(2) Hammond, G. S. *J. Am. Chem. Soc.* **1955**, 77, 334−338.
(3) Leffler, J. E. *Science* **1953**, *117*, 340−341.
(4) Keil, F.; Ahlrichs, R. *J. Am. Chem. Soc.* **1976**, *98*, 4787−4793.
(5) Raghavachari, K.; Chandrasekhar, J.; Burnier, R. C. *J. Am. Chem. Soc.* **1984**, *106*, 3124−3128.

(6) Chandrasekhar, J.; Smith, S. F.; Jorgensen, W. L. *J. Am. Chem. Soc.* **1985**, *107*, 154−163.
(7) Castejon, H.; Wiberg, K. B. *J. Am. Chem. Soc.* **1999**, *121*, 2139−2146.
(8) Kormos, B. L.; Cramer, C. J. *J. Org. Chem.* **2003**, *68*, 6375−6386.
(9) Tondo, D. W.; Pliego, J. R. *J. Phys. Chem. A* **2005**, *109*, 507−511.
(10) Almerindo, G. I.; Pliego, J. R. *Org. Lett.* **2005**, *7*, 1821−1823.
(11) Westphal, E.; Pliego, J. R. *J. Phys. Chem. A* **2007**, *111*, 10068−10074.
(12) Chen, X.; Regan, C. K.; Craig, S. L.; Krenske, E. H.; Houk, K. N.; Jorgensen, W. L.; Brauman, J. I. *J. Am. Chem. Soc.* **2009**, *131*, 16162−16170.
(13) Kim, Y.; Cramer, C. J.; Truhlar, D. G. *J. Phys. Chem. A* **2009**, *113*, 9109−9114.
(14) Ebrahimi, A.; Khorassani, M. H.; Doosti, M. *Int. J. Quantum Chem.* **2012**, *112*, 873−881.
(15) Haddon, R. C.; Chow, S.-Y. *J. Am. Chem. Soc.* **1998**, *120*, 10494−10496.
(16) Frisch, M. J. T.; Trucks, G. W.; Schlegel, H. B.; Scuseria, G. E.; Robb, M. A.; Cheeseman, J. R.; Scalmani, G.; Barone, V.; Mennucci, B.; Petersson, G. A.; Nakatsuji, H.; Caricato, M.; Li, X.; Hratchian, H. P.; Izmaylov, A. F.; Bloino, J.; Zheng, G.; Sonnenberg, J. L.; Hada, M.; Ehara, M.; Toyota, K.; Fukuda, R.; Hasegawa, J.; Ishida, M.; Nakajima, T.; Honda, Y.; Kitao, O.; Nakai, H.; Vreven, T.; Montgomery, J. A., Jr.; Peralta, J. E.; Ogliaro, F.; Bearpark, M.; Heyd, J. J.; Brothers, E.; Kudin, K. N.; Staroverov, V. N.; Keith, T.; Kobayashi, R.; Normand, J.; Raghavachari, K.; Rendell, A.; Burant, J. C.; Iyengar, S. S.; Tomasi, J.; Cossi, M.; Rega, N.; Millam, J. M.; Klene, M.; Knox, J. E.; Cross, J. B.; Bakken, V.; Adamo, C.; Jaramillo, J.; Gomperts, R.; Stratmann, R. E.; Yazyev, O.; Austin, A. J.; Cammi, R.; Pomelli, C.; Ochterski, J. W.; Martin, R. L.; Morokuma, K.; Zakrzewski, V. G.; Voth, G. A.; Salvador, P.; Dannenberg, J. J.; Dapprich, S.; Daniels, A. D.; Farkas, O.; Foresman, J. B.; Ortiz, J. V.; Cioslowski, J.; Fox, D. J. *Gaussian 09*; Gaussian, Inc.: Wallingford, CT, 2009.
(17) Marenich, A. V.; Cramer, C. J.; Truhlar, D. G. *J. Phys. Chem. B* **2009**, *113*, 6378−6396.
(18) Zhao, Y.; Truhlar, D. G. *Acc. Chem. Res.* **2008**, *41*, 157−167.
(19) Zhao, Y.; Truhlar, D. G. *Theor. Chem. Acc.* **2008**, *120*, 215−241.
(20) Hratchian, H. P.; Schlegel, H. B. *J. Chem. Phys.* **2004**, *120*, 9918−9924.
(21) Haddon, R. C. *J. Am. Chem. Soc.* **1986**, *108*, 2837−2842.
(22) Haddon, R. C.; Scott, L. T. *Pure Appl. Chem.* **1986**, *58*, 137−142.
(23) Haddon, R. C. *J. Phys. Chem. A* **2001**, *105*, 4164−4165.
(24) Fersht, R. *Proc. Natl. Acad. Sci. U. S. A.* **2004**, *101*, 14338−14342.
(25) Wurthwein, E.-U.; Lang, G.; Schappele, L. H.; Mayr, H. *J. Am. Chem. Soc.* **2002**, *124*, 4084−4092.
(26) Haddon, R. C.; Chow, S.-Y. *Pure Appl. Chem.* **1999**, *71*, 289−294.
(27) Haddon, R. C. *Acc. Chem. Res.* **1988**, *21*, 243−249.
(28) Haddon, R. C. *Science* **1993**, *261*, 1545−1550.
(29) Niyogi, S.; Hamon, M. A.; Hu, H.; Zhao, B.; Bhowmik, P.; Sen, R.; Itkis, M. E.; Haddon, R. C. *Acc. Chem. Res.* **2002**, *35*, 1105−1113.

■ NOTE ADDED AFTER ASAP PUBLICATION

It is with great sadness that we acknowledge the passing of our colleague and coauthor Robert Haddon just after this paper appeared online, with appreciation for his contributions to this work and all of his career's work.